

Forum Review

Detection of Lipid Radicals Using EPR

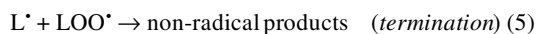
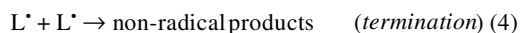
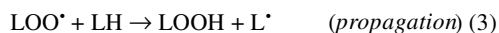
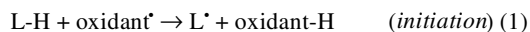
SUJATHA VENKATARAMAN, FREYA Q. SCHAFER, and GARRY R. BUETTNER

ABSTRACT

Cells oxidize molecules to generate energy and to make the materials to build and support the structures and functions needed for life. However, unwanted oxidations can damage these same structures and impair function. Lipids (the lipids in membranes and lipoproteins) are targets of unwanted oxidations. The primary mechanism of these oxidations is free radical-mediated chain reactions. Here we provide an overview of how electron paramagnetic resonance (EPR) can be used to detect the free radicals formed during lipid peroxidation. Although direct detection of lipid-derived radicals has been accomplished, the approach is not feasible for detecting these radicals in cells. Spin trapping with α -(4-pyridyl-1-oxide)-*N*-tert-butyl nitron and 5,5-dimethyl-pyrroline-1-oxide has provided the most information on cellular lipid peroxidation. We present some considerations for successful detection of lipid radicals by EPR. *Antioxid. Redox Signal.* 6, 631–638.

INTRODUCTION

OUR CELLS OXIDIZE molecules or compounds to generate energy and also to make the materials to build and support the structures and functions needed for life. However, unwanted oxidations can damage these same structures and impair function. Lipids, *e.g.*, the lipids in membranes and lipoproteins, are a target of unwanted oxidations. Free radical-mediated lipid peroxidation has three major components: initiation, propagation, and termination reactions (5, 16, 17):



Here L-H represents an unsaturated lipid, generally a polyunsaturated fatty acid (PUFA); L[•] represents a carbon-centered lipid radical; and oxidant[•] represents a radical that has oxidizing properties. The rate of propagation is governed by the various carbon-hydrogen bond dissociation energies in the lipid

chain. PUFAs are especially vulnerable to oxidation because they contain weak carbon-hydrogen bonds (37). The weakest carbon-hydrogen bonds are those of the *bis*-allylic methylene positions that are present in PUFAs. These *bis*-allylic methylene C-H bonds have bond-dissociation energies of approximately 75 kcal/mol compared with 101 kcal/mol for typical alkyl C-H bonds (17, 23) (Fig. 1).

The oxidant in Reaction 1, oxidant[•], can be an oxidizing free radical that has a one-electron reduction potential of greater than approximately +600 mV. This would include HO[•], alkoxyl (RO[•]), peroxy (ROO[•]), HOO[•], and NO₂[•], but not O₂^{•-} or NO[•] radicals.

IRON IN LIPID PEROXIDATION

Iron can be a detrimental participant in lipid peroxidation because it can both initiate (serve as oxidant in Reaction 1) and amplify lipid peroxidation (27). Initiation of lipid peroxidation by iron appears to be by two different mechanisms. Iron(II) can initiate oxidations by reacting with H₂O₂ and thus produce HO[•], a highly oxidizing radical (24). In the HO[•]-dependent mechanism, iron(II) serves as a reagent for the Fenton reaction, forming HO[•], which serves as an oxidant and eventually initiates lipid peroxidation. The HO[•]-dependent

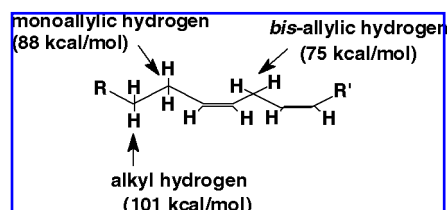


FIG. 1. The types of C-H bonds in lipids. The C-H bonds have widely varying bond dissociation energies.

mechanism has been adopted by most researchers because of the lemming effect. However, an alternate mechanism, HO^\bullet -independent, proposes that iron-oxygen complexes, rather than HO^\bullet from the Fenton reaction, initiate lipid peroxidation (27, 40). In the alternate mechanism, lipid peroxidation is not initiated by HO^\bullet , but rather by iron in the form of iron-oxygen complexes, such as ferryl ion or ferryl ion (see Appendix). Because of the high physiological ratio of $[\text{O}_2]/[\text{H}_2\text{O}_2]$ ($\geq 10^3$), the proposal is that the Fenton reaction with preexisting H_2O_2 is only a minor initiator of free radical oxidations, such as lipid peroxidation. The major initiators of biological free radical oxidations are the oxidizing species formed by the reaction of loosely bound Fe^{2+} with dioxygen (27, 33).

ALKOXYL RADICALS IN LIPID PEROXIDATION

Iron(II) can both initiate lipid peroxidation and bring about chain-branching reactions that amplify these oxidation processes. The chain-branching reactions occur when iron reacts with LOOH, forming PUFA-alkoxyl radicals that can then initiate lipid-derived radical formation (Fig. 2). These alkoxyl radicals have a rich chemistry that results in formation of smaller carbon-centered radicals from β -scission reactions as well as intramolecular addition reactions to form epoxyallylic carbon-centered radicals. All of these carbon-centered radicals will react very rapidly with dioxygen to yield peroxy free radicals. The peroxy radicals formed from epoxy-allylic radicals are considered the major propagators of lipid peroxidation when iron is present (39). Because there is always more than one possible peroxy free radical formed upon initiation, there are many possible radicals formed as the chemistry of these peroxy and alkoxyl radicals proceeds. The detection of these radicals by electron paramagnetic resonance (EPR) can be very informative in understanding the role of lipid peroxidation in issues of human health and disease.

DETECTING LIPID-DERIVED RADICALS BY EPR

Direct detection of radicals formed during lipid peroxidation has been successful where PUFAs, including linoleate and arachidonate, were subjected to lipoxygenase in a rapid-mixing, continuous fast-flow EPR system (7). PUFA-H species

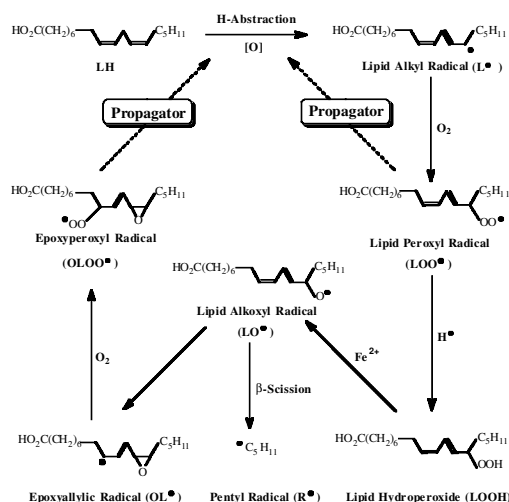


FIG. 2. An overview of the chemistry of the formation of lipid-derived radicals (L_d^\bullet) produced during lipid peroxidation in the presence of ferrous iron. This scheme shows some of the radical species formed in the peroxidation of linoleic acid. Two different propagating species are shown. It is currently thought that OLOO^\bullet may be the major propagating species in this type of system (26, 39). The species LO^\bullet is thought to be a minor propagating species because of its very short lifetime. It is estimated that the rate constant of cyclization of LO^\bullet is approximately $2 \times 10^7 \text{ s}^{-1}$, while the rate constant for β -scission is $\sim 1 \times 10^6 \text{ s}^{-1}$ (18). Scheme adapted from Qian *et al.* (28).

are susceptible to peroxidation because of easily oxidizable bis-allylic hydrogens (5), and therefore peroxy radical ($g = 2.014$; $\Delta H_{\text{pp}} \sim 5\text{--}6 \text{ G}$) was observed with each of the PUFAs examined (7). Although these results provided valuable information on mechanisms of lipid peroxidation, this method of continuous fast-flow technique is not suitable for examining radicals from cells or tissue.

EPR spin trapping has been used to detect a wide variety of radicals from cells and tissues. Spin trapping employs a diamagnetic compound (*the spin trap*) that reacts with a free radical to give a more stable EPR-observable free radical (*the spin adduct*) (Fig. 3). The unstable free radical can then be identified from the EPR spectral parameters, *i.e.*, the hyperfine splitting constants and the g -factor obtained from the spin adduct. In biological systems, spin trapping has been employed for the detection of hydroxyl and superoxide radicals, the study of free radical metabolites of both endogenous substances and xenobiotics, and lipid peroxidation (3, 6, 31). The success of spin trapping experiments lies in the kinetics of the process, both the kinetics of the trapping reaction as well as the lifetime of the resulting spin adduct. 5,5-Dimethyl-pyrroline-1-oxide (DMPO) is a commonly used spin trap because it meets these criteria for a wide variety of radicals, but equally important is that the resulting spin adducts have lifetimes that are long enough to allow accumulation of spin adduct to a concentration that is detectable by standard, continuous-wave EPR approaches. DMPO has provided information on carbon-centered, oxygen-centered, ni-

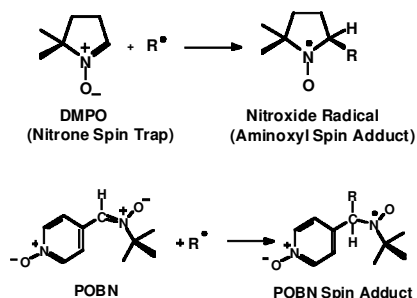


FIG. 3. Example spin trapping reactions. Two spin traps (DMPO and POBN) that have been used in the detection of lipid radicals and their reactions to form spin adducts are shown.

trogen-centered, sulfur-centered, and a variety of other radicals (3, 25). α -(4-Pyridyl-1-oxide)-*N*-*tert*-butylnitron (POBN) also traps oxygen-centered radicals, but their lifetimes are quite short; for example, $t_{1/2}$ of POBN/ HO^\bullet is about 10 s. However, POBN has been very informative in studies of lipid peroxidation because of its ability to trap carbon-centered radicals. It has a good trapping rate constant for carbon-centered radicals, such as those produced during lipid peroxidation (31). A major factor in its advantage for studies of lipid peroxidation stems from the long lifetime of these carbon-centered radical adducts. We have observed that these carbon-centered adducts of POBN have lifetimes of hours and even days in typical near-neutral aqueous solutions, making it a more effective trap than DMPO for carbon-centered radicals. The major shortcoming is that the actual spectra of the various carbon-centered spin adducts are all very much alike. The hyperfine splitting constants are quite

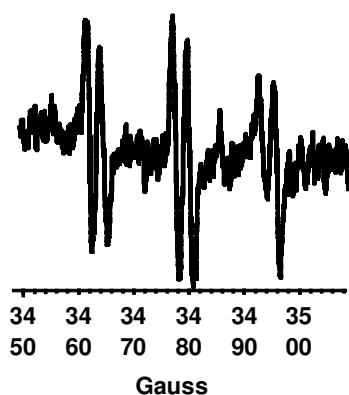


FIG. 4. EPR spectrum of typical carbon-centered POBN spin adducts derived from lipid peroxidation in K562 cells ($a^N = 15.6$ G, $a_\beta^H = 2.6$ G). The cells were grown in RPMI medium with 10% fetal bovine serum supplemented with 32 μ M (DHA) for 48 h. After washing (twice) cells were suspended at a density of 8×10^6 cells/ml, and POBN (25 mM) and then ferrous iron (10 μ M) were added. Prior to this EPR experiment, the DHA-enriched cells were previously exposed to Photofrin and light. Photofrin and light generate singlet oxygen, thereby introducing lipid hydroperoxides into the cell membranes (33). Experimental methods are the same as in Fig. 7.

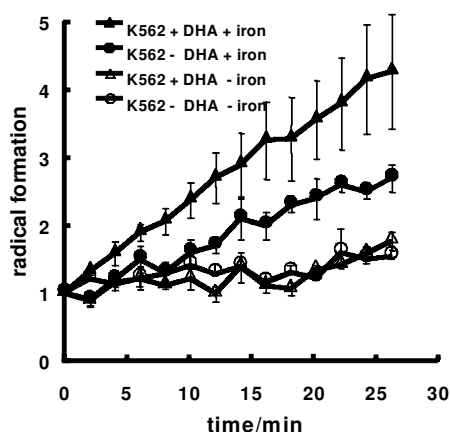


FIG. 5. Increasing the DHA levels in cells enhances lipid peroxidation. Prior to these experiments the K562 cells (with or without DHA) were exposed to Photofrin. Immediately before the EPR experiment POBN (25 mM), ascorbate (100 μ M), and iron as appropriate were introduced to the cell suspension (8×10^6 cells/ml in phosphate-buffered saline, pH 6.5). Solid symbols: Ferrous iron (5 μ M) was added to K562 cells (\bullet) and K562 cells enriched with DHA (\blacktriangle). Open symbols: No ferrous iron was added to K562 cells (\circ) and K562 cells enriched with DHA (\triangle). Desferal was present in these samples to ensure that adventitious iron was inactive. During the EPR experiment, the cells were continuously exposed to light (180 J/m² s), and EPR spectra were continuously recorded. The ordinate represents signal height of the POBN/ L_d^\bullet adduct in arbitrary units. In the absence of light or Photofrin, under these experimental conditions, POBN/ L_d^\bullet remains just at the limit of detection.

similar ($a^N = 15.6$ G, $a_\beta^H = 2.6$ G), and thus a typical EPR spectrum only provides information on the general type of radical, *i.e.*, carbon-centered, and the relative amount trapped (Fig. 4). This type of information can provide many insights into oxidative processes.

Because it is only the PUFAs that participate in free radical-mediated lipid peroxidation, increasing the fatty acid content of cells should make them more susceptible to peroxidation. An example is shown in Fig. 5, where K562 cells were enriched with docosahexaenoic acid (DHA; 22:6) by including it in their growth media. Enriching the growth media with a particular fatty acid results in increasing the cellular content of that fatty acid and its metabolites (37). The amount of DHA incorporated into the cells increased from approximately 3 mol% to 32 mol% of the lipids (33). As seen in Fig. 5, the rate of radical production is greater in cells enriched with DHA compared with those grown in standard media; also, it is clear that iron is an absolute requirement for detectable free lipid radical production in these experiments. These experiments were performed with a low level of Fe(II) (5 μ M). These data are consistent with cells being more oxidizable when they contain greater levels of PUFAs.

Oxidizability of lipids in homogeneous solution varies linearly with the extent of their unsaturation (9). To examine the oxidizability of cells as their lipid profile varies, we measured the rate of production of POBN/ L_d^\bullet (where L_d^\bullet represents a carbon-centered lipid-derived radical) in murine leukemia L-1210 cells exposed to the oxidative stress of iron/ascorbate. After supplementing the growth media with different PUFAs,

we did a total cellular lipid analysis to determine the number of lipid carbon-carbon double bonds contained in L-1210 cells enriched with eight fatty acids of varying degrees of unsaturation. We found in cellular lipids that:

1. Lipid chain length had no apparent effect on the rate or extent of radical formation.
2. The maximum amount of lipid radical generated increases with the total number of *bis*-allylic positions in the cellular lipids.
3. Most importantly, the rate of cellular lipid peroxidation increases exponentially with the number of *bis*-allylic positions (37).

LIPID RADICAL FORMATION INDUCED BY FERROUS IRON CAN BE pH-DEPENDENT

Lipid hydroperoxides formed from unsaturated fatty acids can accumulate in cells during oxidative stress, *e.g.*, singlet oxygen exposure. These lipid hydroperoxides can be by ferrous iron, resulting in formation of oxygen- and carbon-centered lipid radicals. Using EPR and POBN as a spin trap, we have found that iron-induced formation of the lipid-derived radicals from K562 cells is pH-dependent (Fig. 6) (32). When leukemia cells are exposed to a photosensitizer (Photofrin) and light, LOOH is formed *via* singlet oxygen

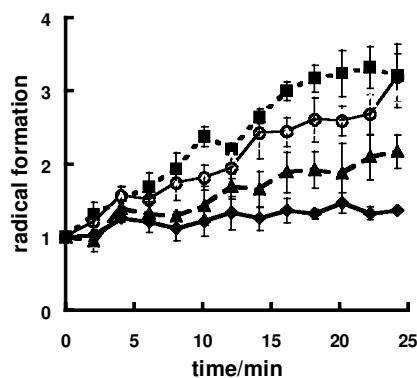


FIG. 6. Lipid radical formation is pH dependent. EPR signal intensity of POBN/ L_d produced from K562 cells is shown. Cells (8×10^6 cells/ml) were treated with Photofrin (9 μ g/ml) for 45 min and then washed and resuspended in phosphate-buffered saline (pH 7.5–6.0): pH 6.0 (■), pH 6.5 (○), pH 7.0 (▲), and pH 7.5 (◆). An aliquot of 500 μ l was mixed with POBN (25 mM), ascorbate (100 μ M), and $FeCl_2$ (5 μ M) and placed into a TM₁₁₀ EPR quartz flat cell. Ferrous iron was used to initiate radical formation from lipid hydroperoxides formed by Photofrin and light. Ascorbate was included to recycle Fe^{3+} back to Fe^{2+} . Cells were exposed to visible light (tungsten, 180 J/m² s) directly in the EPR cavity, and the POBN radical adduct EPR signal intensity was monitored versus time. Each data point represents the signal-averaged result of five scans of the low field doublet of the POBN/lipid-derived radical adduct spectrum. The first five scans were performed in the dark. Experiments were done in triplicates; standard errors are shown.

(21, 36, 38). As seen in Fig. 6, lipid-derived radicals significantly increased when pH values of the media were below 7.4. Changes in the quantum yield of 1O_2 by Photofrin (II) + light in this pH range were minimal. We proposed that because iron is more soluble at acidic pH values, it would be more available for redox reactions. These observations suggest that lipid peroxidation processes, mediated by iron, are enhanced by decreasing extracellular pH.

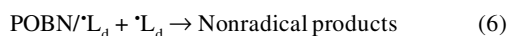
POBN TRAPPING OF L_d

Spectra such as those shown in Fig. 4, collected using standard continuous-wave EPR, can only tell us the type and amount of radical trapped by POBN. The differences in the hyperfine splittings in the various spin adducts do not allow exact identification, especially if more than one carbon-centered radical is trapped. Qian *et al.* have applied a combination of liquid chromatography/EPR, liquid chromatography/mass spectrometry, and tandem mass spectrometry to address this issue (29, 30). Using these combined techniques they have identified various POBN/carbon-centered radical adducts when PUFAs are subjected to lipoxygenase. Linoleate produced 15 EPR-active peaks corresponding to various POBN/ C^* species; arachidonate produced 19 different EPR-active species. The pentyl radical was the dominant radical trapped from both of these fatty acids, consistent with the simplified scheme shown in Fig. 2. This product is expected when oxygen addition (Reaction 2) occurs at C-13 of linoleate (18:2) or C-15 of arachidonate (20:4). It is also possible that oxygen could add to C-9 of 18:2 or C-5,-8,-9,-11,-12 of 20:4. Thus, a myriad of β -scission products are eligible for spin trapping by POBN. The stability of POBN/carbon-centered radical spin adducts has given us a new window to study lipid peroxidation processes in much detail.

EXTRACTION OF SPIN ADDUCTS: DMPO TRAPPING OF L_d

During lipid peroxidation, POBN is an efficient spin trap only for carbon-centered radicals derived from β -scission of lipid alkoxyl radicals. Using DMPO, oxygen-centered lipid radicals have been detected in enzyme-dependent peroxidation reactions (7, 10, 11). We have had some success using DMPO; the EPR spectra show several different species, but spectra are weak, and always changing (28). The difficulties lie in an underappreciated aspect of spin trapping, that is, the resulting spin adduct, a nitroxide, often reacts much faster with free radicals than the original spin trap. For example, superoxide reacts with DMPO with $k_{obs} = 30 M^{-1} s^{-1}$ at pH 7.4 (4). However, the resulting spin adduct, DMPO/OOH, reacts with $O_2^{\cdot-}$ with an estimated rate constant of $5 \times 10^6 M^{-1} s^{-1}$ (4). Similarly, POBN reacts with carbon-centered alkyl radicals to form the nitroxide spin adduct with $k \sim 10^6$ – $10^7 M^{-1} s^{-1}$ (31). In general, peroxy radicals react with nitroxides with rate constants of $10^4 M^{-1} s^{-1}$, while alkyl radicals, such as the carbon-centered radicals produced during lipid peroxidation, react at rates approaching the diffusion-controlled

limit ($k \sim 10^9 \text{ M}^{-1} \text{ s}^{-1}$) (8, 22). These are essentially radical-radical termination reactions that will destroy the spin adducts we wish to observe:



Reaction 6 could be a significant route to the destruction of the spin adducts formed during lipid peroxidation. Also, in our studies of lipid peroxidation, we often have iron present. With respect to the spin adduct, Fe^{2+} is a reductant for the nitroxide, thereby converting it to hydroxylamine. The presence of Fe^{3+} can oxidize nitroxide to oxylamine. In addition, Fe^{2+} induces more radical formation that in turn could destroy spin adduct, especially at low concentrations of oxygen. Hence, the presence of iron can be problematic in spin trapping. Therefore, we reasoned that the destruction of DMPO spin adducts by these alkyl radicals (Reaction 6) could well be a major reason behind the difficulty in the detection of lipid radicals using spin trapping.

Organic extraction has been advantageous in the isolation of lipid-soluble spin adducts (1, 2, 19, 35). We used EPR spin trapping combined with extraction in an attempt to overcome the problem of spin adduct destruction. The extraction process will separate iron (aqueous phase) from the oxidizable lipids (organic phase), thereby slowing or stopping the lipid peroxidation cycle, and consequently slowing the reactions that destroy the spin adducts (Reaction 6).

We have used ethyl acetate to extract the DMPO lipid radical adducts derived from lipid oxidation; we used Folch extraction ($\text{CHCl}_3/\text{CH}_3\text{OH}$, 2:1 vol/vol) for the cell oxidation experiments (15). The organic chloroform layer was separated and evaporated under nitrogen. The radical adduct was then taken up in ethyl acetate (25). The extraction method was used to separate the oxidizable substrates (lipids) from the mediator of oxidation (iron). This separation interrupts the lipid peroxidation processes, thereby stabilizing the $\text{DMPO}/\text{L}_d\cdot$ spin adducts by minimizing Reaction 6. In addition, the extraction dilutes the reactants and products and thereby slows destructive radical-radical reactions. For all experimental models, the lifetimes of DMPO lipid-derived radical adducts post-extraction are much longer (>10 h) than the experimental lifetimes of DMPO radical adducts without extraction (<20 min). Furthermore, combining EPR spin trapping with an extraction process provides the opportunity to detect different types of radical adducts in different phases. Long-chain lipid radicals are detected dominantly in the organic phase, while the small fragment radicals ($\text{R}\cdot$, $\text{HO}\cdot$, $\text{RO}\cdot$) are mostly present in the aqueous phase (28). Extraction will allow the distinguishing of radical adducts *via* their hydrophilic or hydrophobic nature, in addition to their hyperfine splitting constants, permitting identification of radicals that have similar hyperfine splittings, but quite different physical properties.

When linolenic and arachidonic acids were subjected to ferrous iron oxidation in the presence of DMPO, both oxygen and carbon-centered radicals could be observed (Figs. 7 and 8). Each spectrum is a composite of three or four species. Simulation suggests two types of oxygen-centered radicals, tentatively assigned as alkoxyl radicals, and two different carbon-centered radicals. The simulation of these spectra provided a base for analyzing spectra generated when cells are

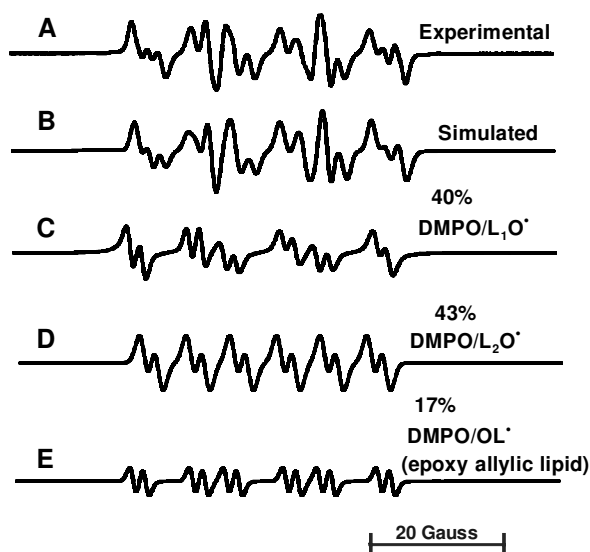


FIG. 7. ESR spectrum of DMPO radical adducts produced by linolenate (18:3) oxidation. Typical experimental conditions were: air-oxidized linolenic acid (5 mM) in phosphate buffer (pH 7.4), incubated with DMPO (50 mM), diethylenediaminepentacetic acid (110 μM), and Fe^{2+} (100 μM). The lipid radical is then extracted by the Folch method (15). The organic phase was extracted into ethyl acetate and transferred to an argon-flushed flat cell, and the ESR spectrum was recorded. The EPR instrument settings were: modulation amplitude, 1.0 G; modulation frequency, 100 kHz; receiver gain, 10^4 – 10^6 . All spectra were simulated using the NIEHS simulation program (14). To assist in the assignment comparisons of splitting constants and g -values were made with published values given in the Spin Trapping Database online at: <http://epr.niehs.nih.gov/stdb1.html>. **A:** Experimental EPR spectrum of DMPO-lipid radical adduct of oxidized linolenic acid in the organic phase. **B:** Composite computer-simulated spectrum of **A**. **C:** Computer simulation of $\text{DMPO}/\text{L}_1\text{O}\cdot$ radical adduct of spectrum **A** with $\text{DMPO}/\text{LOO}\cdot$ with $a^{\text{N}} = 13.13 \text{ G}$, $a_{\beta}^{\text{H}} = 10.59 \text{ G}$, $a_{\gamma}^{\text{H}} = 1.34 \text{ G}$ (40%). The $\text{DMPO}/\text{L}_1\text{O}\cdot$ adduct results from the conversion of the first formed product (13). **D:** Computer-simulated spectrum of $\text{DMPO}/\text{L}_2\text{O}\cdot$ radical adduct of spectrum **A** using the parameters $a^{\text{N}} = 13.28 \text{ G}$, $a_{\beta}^{\text{H}} = 6.88 \text{ G}$, $a_{\gamma}^{\text{H}} = 2.0 \text{ G}$ (43%). **E:** Computer simulation of $\text{DMPO}/\text{OL}\cdot$, an epoxy allylic radical adduct of spectrum **A** with $a^{\text{N}} = 13.74 \text{ G}$, $a_{\beta}^{\text{H}} = 8.75 \text{ G}$, $a_{\gamma}^{\text{H}} = 1.83 \text{ G}$ (17%). $\text{L}_1\text{O}\cdot$ and $\text{L}_2\text{O}\cdot$ are the two diastereomers of the DMPO/PUFA -alkoxyl radical adducts (13). A very small signal (<1%) consistent with a carbon-centered radical being trapped, $\text{DMPO}/\text{L}\cdot$, as shown in Fig. 8F, is also present.

subjected to the oxidative stress of ferrous iron (Figs. 9 and 10). When DMPO and the extraction approach were used to detect lipid-derived free radicals from the prostate cancer cell line PC-3, three different patterns from the EPR spectra were consistently observed. Simulation of these three spectra demonstrated that they resulted from different proportions of the same basic set of spectra. All spectra were simulated using hyperfine values reported for individual components that are generated independently (12, 13, 20, 34). Figure 10 shows the results of the simulation of spectra shown in Fig. 9A and B. Although these results are not yet totally understood, they provide us with an approach for the detection of radicals pro-

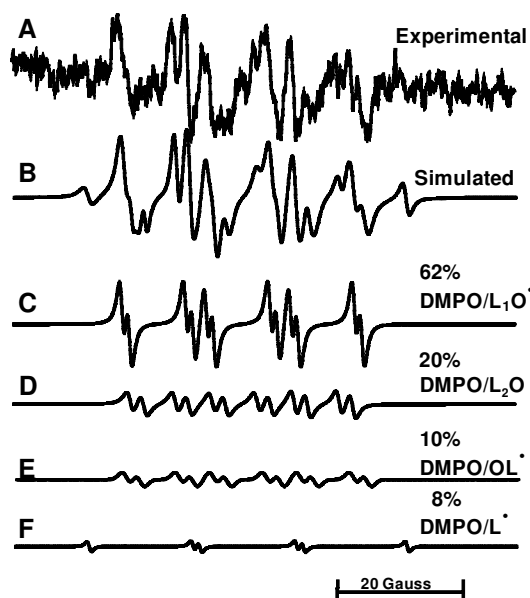


FIG. 8. ESR spectrum of DMPO/lipid radical adduct formed from the Fe^{2+} -mediated oxidation of DHA in aerobic conditions. **A:** Experimental ESR spectrum of lipid radical adducts of DMPO in ethyl acetate formed during oxidation of DHA (22:6). **B:** Composite computer-simulated spectrum of **A**. **C:** Computer-simulated spectrum of radical adducts of $\text{DMPO/L}_1\text{O}^\bullet$ (62%). **D:** $\text{DMPO/L}_2\text{O}^\bullet$ (20%). **E:** DMPO/OL^\bullet (10%). **F:** DMPO/L^\bullet (8%) with $a^N = 15.10$ G, $a_\beta^H = 22.36$ G components of spectrum **A**. The hyperfine splitting constant values of other species are as given in the legend of Fig. 7. Experimental methods and instrumental settings were as in Fig. 7.

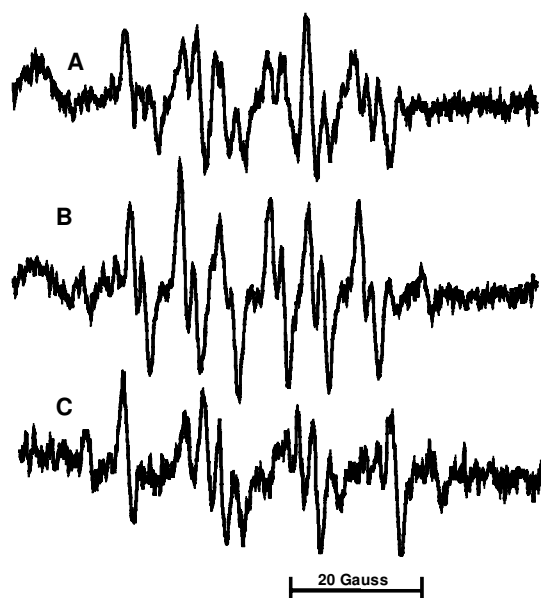


FIG. 9. Representative ESR spectra of DMPO lipid radical adduct formed from PC-3 prostate cancer cells. The ESR spectra of radicals were obtained using the combination of ESR and Folch extraction after the cells (1.5×10^6) were incubated with DMPO (150 mM), diethylenediaminepentaacetic acid (110 μM), and Fe^{2+} (100 μM). All spectra are the result of 40 signal-averaged scans. **A–C:** These three different ESR spectral patterns were obtained repeatedly from this system. They mostly represent differing contributions from each species present. The reasons for these differences are not yet known.

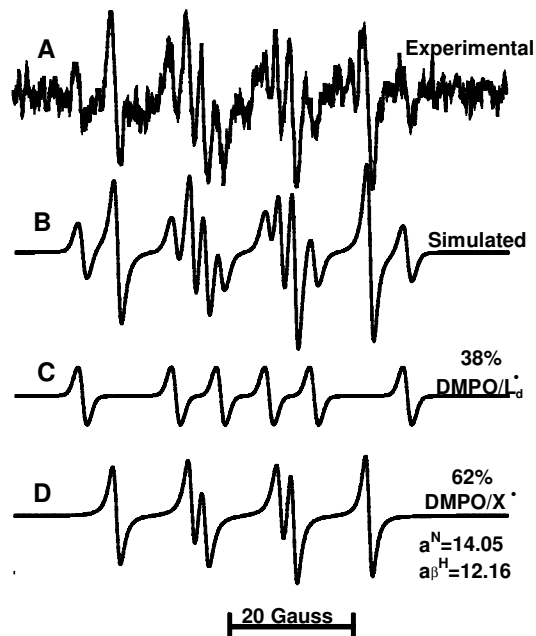
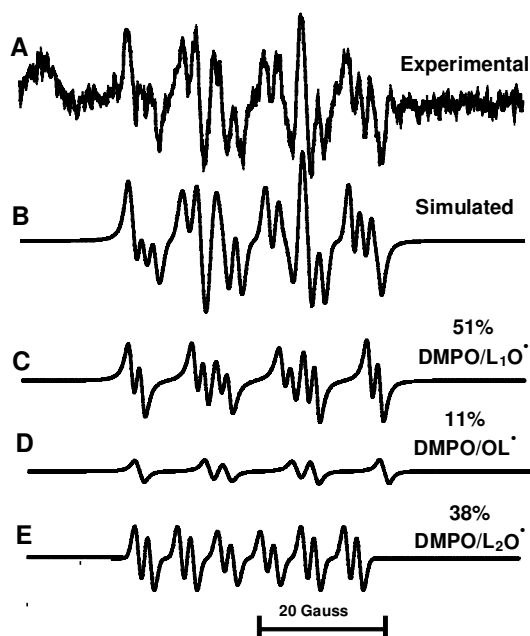


FIG. 10. Spectral simulation of experimental spectra obtained from the PC-3 cell lipid radical adducts. **a:** Experimental spectral pattern of Fig. 9A (**A**), computer-simulated spectrum of **A** (**B**), computer-simulated spectrum of radical adducts of $\text{DMPO/L}_1\text{O}^\bullet$ (51%) (**C**), DMPO/OL^\bullet (11%) (**D**), and $\text{DMPO/L}_2\text{O}^\bullet$ (38%) (**E**). **b:** Experimental spectral pattern of Fig. 9C (**A**), composite computer-simulated spectrum of **A** (**B**), and computer-simulated components of **A** corresponding to DMPO/L^\bullet (38%) (**C**) and an unknown component of **A** corresponding to DMPO/X^\bullet with $a^N = 14.05$ G, $a_\beta^H = 12.16$ G (62%) (**D**).

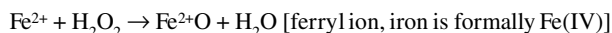
duced during lipid peroxidation in cells and tissues that complements those detected with POBN.

SUMMARY

Unsaturated lipids are the targets for the free radical-mediated oxidations. Iron(II) together with dioxygen can be the initiating agents for lipid peroxidation in cells. The detection of the free radicals generated during lipid peroxidation can be best accomplished by EPR spin trapping. POBN is an excellent spin trap to detect the carbon-centered radicals generated. DMPO is able to capture some of the oxygen-centered radicals produced, but the signals are weak and dynamic; extraction approaches with DMPO provide a window to observe the spin adducts.

APPENDIX

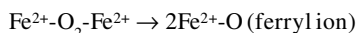
Ferryl ion is thought to be formed by two routes:



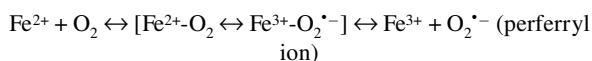
or



then,



Perferryl iron is an intermediate product that produced through either $\text{Fe}^{2+}/\text{O}_2$ or $\text{Fe}^{3+}/\text{O}_2^{\bullet-}$:



ACKNOWLEDGMENTS

We thank Mr. Sean Martin for his help in preparing this article. This work was supported by NIH grants CA-66081, CA84462, and CA-81090.

ABBREVIATIONS

DHA, docosahexaenoic acid (22:6); DMPO, 5,5-dimethylpyrroline-1-oxide; EPR, electron paramagnetic resonance; L-H, unsaturated lipid; L^{\bullet} , carbon-centered lipid radical; L_d^{\bullet} , carbon-centered lipid-derived radical; oxidant $^{\bullet}$, a radical that has oxidizing properties; POBN, α -(4-pyridyl)-1-oxide)-*N*-tert-butyl nitron; PUFA, polyunsaturated fatty acid.

REFERENCES

- Albano E, Lott KA, Slater TF, Stier A, Symons MC, and Tomasi A. Spin-trapping studies on the free-radical products formed by metabolic activation of carbon tetrachloride in rat liver microsomal fractions isolated hepatocytes and in vivo in the rat. *Biochem J* 204: 593–603, 1982.
- Bolli R and McCay PB. Use of spin traps in intact animals undergoing myocardial ischemia/reperfusion: a new approach to assessing the role of oxygen radicals in myocardial “stunning.” *Free Radic Res Commun* 9: 169–180, 1990.
- Buettner GR. Spin trapping: ESR parameters of spin adducts. *Free Radic Biol Med* 3: 259–303, 1987.
- Buettner GR. On the reaction of superoxide with DMPO/OOH. *Free Radic Res Commun* 10: 11–15, 1990.
- Buettner GR. The pecking order of free radicals and antioxidants: lipid peroxidation, α -tocopherol and ascorbate. *Arch Biochem Biophys* 300: 535–543, 1993.
- Buettner GR and Mason RP. Spin-trapping methods for detecting oxygen-derived radical formation *in vitro* and *in vivo*. *Methods Enzymol* 186: 127–133, 1990.
- Chamulitrat W and Mason RP. Lipid peroxy radical intermediates in the peroxidation of polyunsaturated fatty acids by lipoxygenase: direct electron spin resonance investigations. *J Biol Chem* 264: 20968–20973, 1989.
- Chateaufort J, Luszyk J, and Ingold KU. Absolute rate constants for the reaction of some carbon-centered radicals with 2,2,6,6-tetramethylpiperidine-N-oxyl. *J Org Chem* 53: 1629–1632, 1988.
- Cosgrove JP, Church DF, and Pryor WA. The kinetics of the autoxidation of polyunsaturated fatty-acids. *Lipids* 22: 299–304, 1987.
- Davies MJ. Detection of peroxy and alkoxy radicals produced by reaction of hydroperoxides with heme-proteins by electron spin resonance spectroscopy. *Biochim Biophys Acta* 964: 28–35, 1988.
- Davies MJ and Slater TF. Studies on the metal-ion and lipoxygenase-catalysed breakdown of hydroperoxides using electron-spin-resonance spectroscopy. *Biochem J* 245: 167–173, 1987.
- Dikalov SI and Mason RP. Reassignment of organic peroxy radical adduct. *Free Radic Biol Med* 27: 864–872, 1999.
- Dikalov SI and Mason RP. Spin trapping of PUFA-derived peroxy radical: reassignment to alkoxy radical adduct. *Free Radic Biol Med* 30: 187–197, 2001.
- Duling DR. Simulation of multiple isotropic spin trap EPR-spectra. *J Magn Reson B* 104: 105–110, 1994.
- Folch J, Lees M, and Stanley GHS. A simple method for the isolation and purification of total lipids from animal tissues. *J Biol Chem* 226: 497–509, 1957.
- Frankel EN. *Lipid Oxidation*. Dundee, Scotland: The Oily Press, 1998.
- Gardner HW. Oxygen radical chemistry of polyunsaturated fatty acids. *Free Radic Biol Med* 7: 65–86, 1989.
- Grossi L, Strazzari S, Gilbert BC, and Whitwood AC. Oxiranylcarbinyl radicals from allyloxy radical cyclization: characterization and kinetic information via ESR spectroscopy. *J Org Chem* 63: 8366–8372, 1998.
- Janzen EG, Townner RA, and Haire DL. Detection of free radicals generated from the *in-vitro* metabolism of carbon tetrachloride using improved ESR spin trapping techniques. *Free Rad Res Commun* 3: 357–364, 1987.
- Kalyanaraman B, Mottley C, and Mason RP. On the use of organic extraction in the spin trapping technique as applied to biological systems. *J Biochem Biophys Methods* 9: 27–31, 1984.

21. Keene JP, Kessel D, Land EJ, Redmond RW, and Truscott TG. Direct detection of singlet oxygen sensitized by haematoporphyrin and related compounds. *Photochem Photobiol* 43: 117–20, 1986.
22. Kocherginsky N and Swartz HM. Chemical reactivity of nitroxides. In: *Nitroxide Spin Labels: Reactions in Biology and Chemistry*, edited by Kocherginsky N and Swartz HM. Boca Raton, FL: CRC Press, 1995, pp. 48–49.
23. Koppenol WH. The Haber-Weiss cycle—70 years later. *Redox Rep* 6: 229–234, 2001.
24. Koppenol WH. Oxyradical reactions: from bond-dissociation energies to reduction potentials. *FEBS Lett* 264: 165–167, 1990.
25. Li ASW, Cummings KB, Roethling HP, Buettner GR, and Chignell CF. A spin trapping data base implemented on the IBM PC/AT. *J Magn Reson* 79: 140–142, 1988. Online at: <http://eprniehs.nih.gov/stdb.html> or <http://www.chm.bris.ac.uk/stdb/index.html>
26. Marnett LJ and Wilcox AL. The chemistry of lipid alkoxyl radical and their role in metal-amplified lipid peroxidation. *Biochem Soc Symp* 61: 65–72, 1996.
27. Qian SY and Buettner GR. Iron and dioxygen chemistry is an important route to initiation of biological free radical oxidations: an electron paramagnetic resonance spin trapping study. *Free Radic Biol Med* 26: 1447–1456, 1999.
28. Qian SY, Wang HP, Schafer FQ, and Buettner GR. EPR detection of lipid-derived radicals from PUFA, LDL, and cell oxidations. *Free Radic Biol Med* 29: 568–579, 2000.
29. Qian SY, Tomer KB, Yue GH, Guo Q, Kadiiska MB, and Mason RP. Characterization of the initial carbon-centered pentadienyl radical and subsequent radicals in lipid peroxidation: identification via on-line high performance liquid chromatography/electron spin resonance and mass spectrometry. *Free Radic Biol Med* 33: 998–1009, 2002.
30. Qian SY, Yue GH, Tomer KB, and Mason RP. Identification of all classes of spin-trapped carbon-centered radicals in soybean lipoxygenase-dependent lipid peroxidations of -6 polyunsaturated fatty acids via LC/ESR, LC/MS, and tandem MS. *Free Radic Biol Med* 34: 1017–1028, 2003.
31. Rosen GM, Britigan BE, Halpern HJ, and Pou S. *Free Radicals: Biology and Detection by Spin Trapping*. New York: Oxford University Press, 1999.
32. Schafer FQ and Buettner GR. Acidic pH amplifies iron-mediated lipid peroxidation in cells. *Free Radic Biol Med* 28: 1175–1181, 2000.
33. Schafer FQ, Qian SY, and Buettner GR. Iron and free radical oxidations in cell membranes. *Cell Mol Biol* 46: 657–662, 2000.
34. Schaich KM and Borg DC. Fenton reactions in lipid phases. *Lipids* 23: 570–579, 1988.
35. Schaich KM and Borg DC. Solvent effects in the spin trapping of lipid oxyl radicals. *Free Radic Res Commun* 9: 267–278, 1990.
36. Thomas JP, Hall RD, and Girotti AW. Singlet oxygen intermediacy in the photodynamic action of membrane-bound hematoporphyrinderivative. *Cancer Lett* 35: 295–302, 1987.
37. Wagner BA, Buettner GR, and Burns CP. Free radical-mediated peroxidation in cells: Oxidizability is a function of cell lipid bis-allylic hydrogen content. *Biochemistry* 33: 4449–4453, 1994.
38. Wang HP, Qian SY, Schafer FQ, Domann FE, Oberley LW, and Buettner GR. Phospholipid hydroperoxide glutathione peroxidase protects against the singlet oxygen-induced cell damage of photodynamic therapy. *Free Radic Biol Med* 30: 825–835, 2001.
39. Wilcox AL and Marnett LJ. Polyunsaturated fatty acid alkoxyl radicals exist as carbon-centered epoxyallylic radicals: a key step in hydroperoxide-amplified lipid peroxidation. *Chem Res Toxicol* 6: 413–416, 1993.
40. Yin D, Lingnert H, Ekstrand B, and Brunk UT. Fenton reagents may not initiate lipid peroxidation in emulsified linoleic acid model system. *Free Radic Biol Med* 13: 543–556, 1992.

Address reprint requests to:

Dr. Garry R. Buettner

Free Radical and Radiation Biology Program

EMRB 68

The University of Iowa

Iowa City, IA 52242-1101

E-mail: garry-buettner@uiowa.edu

Received for publication July 8, 2003; accepted February 19, 2004.

This article has been cited by:

1. Yanfei Li, Shimin Liu. 2012. Reducing lipid peroxidation for improving colour stability of beef and lamb: on-farm considerations. *Journal of the Science of Food and Agriculture* **92**:4, 719-729. [[CrossRef](#)]
2. Nathan R. Perron, Carla R. García, Julio R. Pinzón, Manuel N. Chaur, Julia L. Brumaghim. 2011. Antioxidant and prooxidant effects of polyphenol compounds on copper-mediated DNA damage. *Journal of Inorganic Biochemistry* **105**:5, 745-753. [[CrossRef](#)]
3. S.M. Liu, H.X. Sun, C. Jose, A. Murray, Z.H. Sun, J.R. Briegel, R. Jacob, Z.L. Tan. 2011. Phenotypic blood glutathione concentration and selenium supplementation interactions on meat colour stability and fatty acid concentrations in Merino lambs. *Meat Science* **87**:2, 130-139. [[CrossRef](#)]
4. Wanvimol Pasanphan, Garry R. Buettner, Suwabun Chirachanchai. 2010. Chitosan gallate as a novel potential polysaccharide antioxidant: an EPR study. *Carbohydrate Research* **345**:1, 132-140. [[CrossRef](#)]
5. Natalia A. Belikova, Yulia Y. Tyurina, Grigory Borisenko, Vladimir Tyurin, Alejandro K. Samhan Arias, Naveena Yanamala, Paul Georg Furtmu#ller, Judith Klein-Seetharaman, Christian Obinger, Valerian E. Kagan. 2009. Heterolytic Reduction of Fatty Acid Hydroperoxides by Cytochrome c / Cardiolipin Complexes: Antioxidant Function in Mitochondria. *Journal of the American Chemical Society* **131**:32, 11288-11289. [[CrossRef](#)]
6. W PASANPHAN, S CHIRACHANCHAI. 2008. Conjugation of gallic acid onto chitosan: An approach for green and water-based antioxidant. *Carbohydrate Polymers* **72**:1, 169-177. [[CrossRef](#)]
7. Yukihiko Hama , Ken-Ichiro Matsumoto , Ramachandran Murugesan , Sankaran Subramanian , Nallathamby Devasahayam , Janusz W. Koscielniak , Fuminori Hyodo , John A. Cook , James B. Mitchell , Murali C. Krishna . 2007. Continuous Wave EPR Oximetric Imaging at 300 MHz Using Radiofrequency Power Saturation Effects. *Antioxidants & Redox Signaling* **9**:10, 1709-1716. [[Abstract](#)] [[Full Text PDF](#)] [[Full Text PDF with Links](#)]
8. Griselda R. Borthiry, William E. Antholine, B. Kalyanaraman, Judith M. Myers, Charles R. Myers. 2007. Reduction of hexavalent chromium by human cytochrome b5: Generation of hydroxyl radical and superoxide. *Free Radical Biology and Medicine* **42**:6, 738-755. [[CrossRef](#)]
9. Angel Catalá. 2006. An overview of lipid peroxidation with emphasis in outer segments of photoreceptors and the chemiluminescence assay. *The International Journal of Biochemistry & Cell Biology* **38**:9, 1482-1495. [[CrossRef](#)]
10. Sascha Rohn, Lothar W. Kroh. 2005. Electron spin resonance - A spectroscopic method for determining the antioxidative activity. *Molecular Nutrition & Food Research* **49**:10, 898-907. [[CrossRef](#)]
11. Periannan Kuppusamy . 2004. EPR Spectroscopy in Biology and Medicine. *Antioxidants & Redox Signaling* **6**:3, 583-585. [[Citation](#)] [[Full Text PDF](#)] [[Full Text PDF with Links](#)]